© 2000 The Chemical Society of Japan

Magnetic Properties of the Octahedral Chromium Chalcogenide Cluster Complexes $[Cr_6Se_8(PEt_3)_6]$, $[Cr_6Se_8(H)(PEt_3)_6]$, and $[Cr_6S_8(H)(PEt_3)_6]$

Satoshi Kamiguchi,* Taro Saito,† and Wasuke Mori†

The Institute of Physical and Chemical Research (RIKEN), Wako-shi, Saitama 351-0198

†Department of Chemistry, Faculty of Science, Kanagawa University, Hiratsuka-shi, Kanagawa 259-1293

(Received May 10, 2000)

The magnetic data of chromium chalcogenide cluster complexes $[Cr_6Se_8(PEt_3)_6]$ (**1**), $[Cr_6Se_8(H)(PEt_3)_6]$ (**2**), and $[Cr_6S_8(H)(PEt_3)_6]$ (**3**) have been analyzed using the Heisenberg–Dirac–Van Vleck Hamiltonian. The analysis has shown that all of these complexes display an antiferromagnetic interaction between chromium atoms and that the coupling constants decrease in the order **2** > **3** > **1**. This interaction is mediated by Cr–(μ_3-E)–Cr bridges (E = Se, S) and Cr–Cr bonds. In a comparison of the two hydride clusters, the selenide **2** has a larger antiferromagnetic coupling than the sulfide **3**. The shorter Cr–Cr distances in **2** (mean 2.66 Å) than those in **1** (mean 2.81 Å) seem to cause larger antiferromagnetic interaction through the Cr–Cr bonds.

In studies of metal cluster complexes, their properties based on a metal–metal bonding interaction and their multinuclear nature have attracted much attention. The metal–metal bonds in 3d-metal cluster complexes are weaker than those in 4d- or 5d-metal ones because the 3d orbitals are less expanding. Thus, 3d-metal cluster complexes display very different properties from those of 4d- or 5d-metal cluster complexes. This difference is apparent regarding the magnetic properties. Since 3d-metal cluster complexes have weak metal–metal bonds, the energy gaps between the ground and excited states are small. Therefore, some 3d-metal cluster complexes do not obey the Curie law, but show a significant thermal variation in the number of unpaired electrons (temperature-dependent paramagnetism).[1—5] In these complexes, a spin–spin interaction takes place through metal–metal bonds and bridging ligands synergically.

In spite of such interesting magnetic behaviors in 3d-metal cluster complexes, there have been only a few reports on their magnetism,[2—11] and the relation between the structures and the magnetic properties is still not very clear. Temperature-dependent paramagnetism has also been observed for many polynuclear complexes without metal–metal bonds, and their magnetic behaviors have been theoretically investigated using a calculation with the Heisenberg–Dirac–Van Vleck (HDVV) Hamiltonian.[12] By introducing this theoretical calculation to the cluster complexes, the magneto-structural correlation in 3d-metal cluster complexes will be clarified more significantly.

We have reported chromium cluster complexes $[Cr_6Se_8(PEt_3)_6]$ (**1**), $[Cr_6Se_8(H)(PEt_3)_6]$ (**2**), and $[Cr_6S_8(H)(PEt_3)_6]$ (**3**).[13,14] These complexes have a Cr_6E_8 (E = S, Se) cluster unit consisting of a Cr_6 octahedron and eight face-capping E atoms; complexes **2** and **3** have an interstitial hydrogen atom (Fig. 1). All of these complexes are paramagnetic, and the magnetic susceptibilities do not obey the Curie law. We have analyzed the magnetic data of these complexes by using the HDVV Hamiltonian.

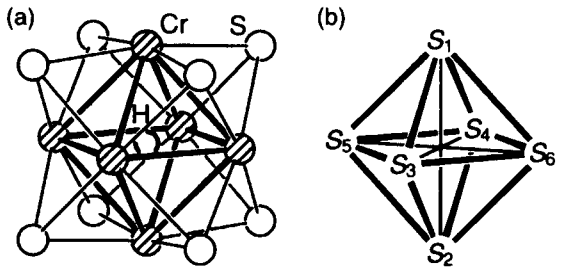

Fig. 1. (a) The structure of the $Cr_6S_8(H)$ cluster unit in **3**. (b) Schematic view of the spin–spin magnetic interaction in complexes **1**, **2**, and **3**. Bold lines represent *cis*-interaction with 2*J* value.

Experimental

Preparations. Complexes **1**, **2**, and **3** were prepared by following the reported procedures.[13] Since crystals of **2** contained THF molecules escaping from them, they were dried in vacuo at 70 °C to completely remove THF.

Magnetic Measurements. The magnetic susceptibilities of **1**, **2**, and **3** were measured in the temperature ranges 2.0—350 K, 2.5—350 K, and 4.5—330 K, respectively, with a Quantum Design MPMS SQUID magnetometer. The absence of ferromagnetic impurities was checked by a magnetization measurements at 300 K. The magnetic field of the measurements was 100 G over the whole measured temperature range for **1**, and 5 kG in the temperature range 4.5—30 K and 10 kG in the range 30—330 K for **2** and **3**, where the magnetization versus magnetic field curves were linear. The crystalline samples (ca. 30 mg for **1**, ca. 90 mg for **2**, and ca. 100 mg for **3**) were filled in cellophane sample holders under a nitrogen atmosphere. The magnetic susceptibilities of the holders were determined separately. Diamagnetic corrections were

estimated from Pascal's constants.[15]

Fitting Calculations. All calculations were performed on a GATEWAY 2000 computer. The programs for calculating the energy levels of the spin states and for the non-linear least-squares fittings were made with turbo-pascal software and Maple V release 4 software, respectively.

Results

The measured temperature dependence of the molar magnetic susceptibilities (χ_M) and the effective magnetic moments (μ_{eff}) of **1**, **2**, and **3** are shown as plots in Figs. 2, 3, and 4, respectively. The magnetic moments of all these complexes do not obey the Curie law, and the μ_{eff} values decrease upon lowering the temperature. Complex **1** has an even number of cluster valence electrons (80 e). Since the μ_{eff} value at 2.0 K is 0.2 μ_B, it is reasonable to assume that the number of unpaired spins approaches zero at very low temperatures, and that $S = 0$ becomes the ground state near 0 K. On the other hand, complexes **2** and **3** have an odd number of cluster valence electrons (81 e). The μ_{eff} values

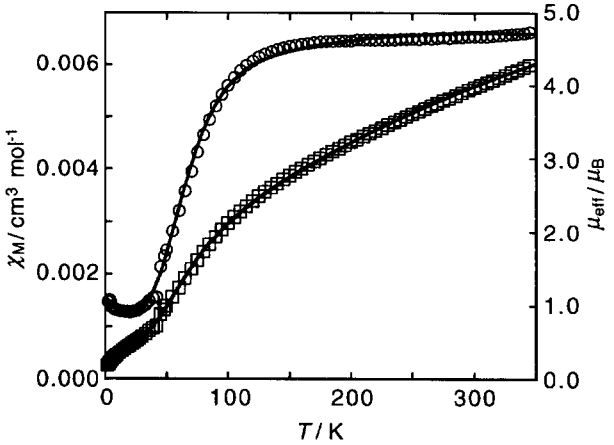

Fig. 2. Temperature dependence of experimental molar magnetic susceptibility (○) and effective magnetic moment (□) for **1**. The solid lines are the calculated values using the best-fit parameters given in Table 1.

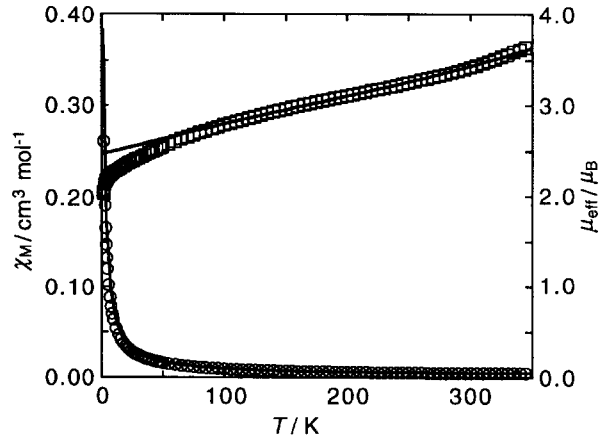

Fig. 3. Temperature dependence of experimental molar magnetic susceptibility (○) and effective magnetic moment (□) for **2**. The solid lines are the calculated values using the best-fit parameters given in Table 1.

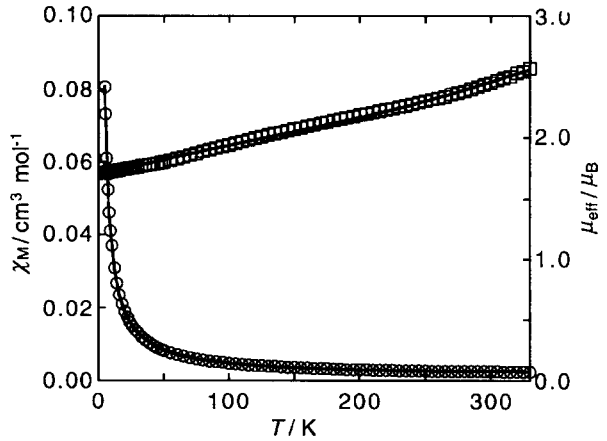

Fig. 4. Temperature dependence of experimental molar magnetic susceptibility (○) and effective magnetic moment (□) for **3**. The solid lines are the calculated values using the best-fit parameters given in Table 1.

for **2** at 2.5 K (2.1 μ_B) and for **3** at 4.5 K (1.7 μ_B) are close to 1.73 μ_B, corresponding to one unpaired spin, indicating that $S = 1/2$ should be the ground state.

Because the Cr_6 octahedra are almost regular, as indicated by X-ray structure determinations,[13,14] these complexes have only two topologically distinct types of exchange interactions: (i) between *trans*-chromium atoms (the *trans*-interaction) and (ii) between *cis*-chromium atoms (the *cis*-interaction) (Fig. 1b). The *trans*-interaction is very weak because it is mediated by no atom in **1** and by only one interstitial hydrogen atom in **2** and **3**, while the *cis*-interaction is effectively transmitted through Cr–(μ_3-chalcogen)–Cr bridges and Cr–Cr bonds. Thus, the *trans*-interaction has been neglected and only the *cis*-interaction has been taken into consideration. The spin Hamiltonian can be formulated as follows (Eq. 1):

$$H = -2J(\boldsymbol{S}_1\cdot\boldsymbol{S}_3 + \boldsymbol{S}_3\cdot\boldsymbol{S}_2 + \boldsymbol{S}_2\cdot\boldsymbol{S}_4 + \boldsymbol{S}_4\cdot\boldsymbol{S}_1 + \boldsymbol{S}_1\cdot\boldsymbol{S}_6 + \boldsymbol{S}_6\cdot\boldsymbol{S}_2 + \boldsymbol{S}_2\cdot\boldsymbol{S}_5 + \boldsymbol{S}_5\cdot\boldsymbol{S}_1 + \boldsymbol{S}_3\cdot\boldsymbol{S}_6 + \boldsymbol{S}_6\cdot\boldsymbol{S}_4 + \boldsymbol{S}_4\cdot\boldsymbol{S}_5 + \boldsymbol{S}_5\cdot\boldsymbol{S}_3), \quad (1)$$

where $2J$ corresponds to the interaction between *cis*-chromium atoms. By defining $\boldsymbol{S}_{12} = \boldsymbol{S}_1 + \boldsymbol{S}_2$, $\boldsymbol{S}_{34} = \boldsymbol{S}_3 + \boldsymbol{S}_4$, $\boldsymbol{S}_{56} = \boldsymbol{S}_5 + \boldsymbol{S}_6$, $\boldsymbol{S}^* = \boldsymbol{S}_{12} + \boldsymbol{S}_{34}$, and $\boldsymbol{S}_T = \boldsymbol{S}^* + \boldsymbol{S}_{56}$, the Hamiltonian (Eq. 1) is rewritten as

$$H = -J(S_T^2 - S_{12}^2 - S_{34}^2 - S_{56}^2). \quad (2)$$

Since the eigenvalues of S_{ij}^2, S^{*2}, and S_T^2 are $S_{ij}(S_{ij} + 1)$, $S^*(S^* + 1)$, and $S_T(S_T + 1)$, respectively, the energy levels E are given by

$$E(S_T, S_{12}, S_{34}, S_{56}) = -J[S_T(S_T + 1) - S_{12}(S_{12} + 1) - S_{34}(S_{34} + 1) - S_{56}(S_{56} + 1)]. \quad (3)$$

(S_{ij} varies from $|S_i + S_j|$ to $|S_i - S_j|$, S^* from $|S_{12} + S_{34}|$ to $|S_{12} - S_{34}|$, and S_T from $|S^* + S_{56}|$ to $|S^* - S_{56}|$ in integer increments.)

All of the compounds are in a mixed-valence state. Complex **1** has two Cr^{II} and four Cr^{III} ions, whereas there are one Cr^{II} and five Cr^{III} centers for **2** and **3** when the interstitial

hydrogen atoms are regarded as H^-.[16] The Cr^{III} ions have $S = 3/2$, while the Cr^{II} centers are assumed to be in the high-spin $S = 2$ state, because the low-spin chromium(II) complexes are rare and limited to those with such ligands as 2,2′-bipyridine, 1,10-phenanthroline, or CN^-, which exert very strong ligand fields.[17]

Complex **1** is either a *cis*-isomer or a *trans*-isomer in which two Cr^{II} sites are placed at the *cis* or *trans* positions, respectively. Thus, fitting calculations have been performed for these isomers separately. The S_{ij}, S^* and S_T values of the *cis*-isomer can be obtained by setting $S_1 = S_3 = 2$ and $S_2 = S_4 = S_5 = S_6 = 3/2$, and those of the *trans*-isomer by setting $S_1 = S_2 = 2$ and $S_3 = S_4 = S_5 = S_6 = 3/2$. On the other hand, there is no isomer of **2** or **3**. The S_{ij}, S^*, and S_T values of these complexes are given by setting $S_1 = 2$ and $S_2 = S_3 = S_4 = S_5 = S_6 = 3/2$. After substituting S_{ij}, S^*, and S_T values of **1**, **2**, and **3** to Eq. 3, the obtained energy levels E (S_T, S_{12}, S_{34}, S_{56}) of each complex are inserted into the Van Vleck formula, including the contribution of temperature-independent paramagnetism (TIP). Since complex **1** exhibits an increase in the χ_M values at lower temperatures, the presence of an impurity obeying the Curie law ($S = 1/2$) was also taken into consideration in the analysis for **1**. Thus, the theoretical magnetic susceptibility of **1**, **2**, and **3** is given as follows (Eq. 4):

$$\chi_M = \frac{N\mu_B^2 g^2}{3kT} \frac{\sum_{S_T} S_T(S_T+1)(2S_T+1)e^{-E(S_T,S_{12},S_{34},S_{56})/kT}}{\sum_{S_T}(2S_T+1)e^{-E(S_T,S_{12},S_{34},S_{56})/kT}}(1-\rho) + \frac{N\mu_B^2 g^2 \rho}{4kT} + N\alpha, \quad (4)$$

where μ_B, g, and $N\alpha$ are the Bohr magneton, the g-factor, and the temperature-independent paramagnetism, respectively, and N, k, and T have their usual meanings. The fraction of paramagnetic impurity present is represented by ρ, which was fixed at 0 for **2** and **3**. Non-linear least-squares fittings of the theoretical expression to the experimental data for **1**, **2**, and **3** were made by varying g, $2J$, ρ (only for **1**), and $N\alpha$ and by minimizing the residual $R = [\sum(\chi_{obs.} - \chi_{calc.})^2 / \sum(\chi_{obs.})^2]$.

Complex **1** showed satisfactory least-squares fits. The best-fit parameters are as follows: $g = 1.973(6)$, $2J = -174.7(10)$ cm^{-1}, $\rho = 0.0016(5)$, and $N\alpha = 0.00128(3)$ $cm^3\ mol^{-1}$ for the *cis*-isomer; $g = 1.993(2)$, $2J = -176.7(8)$ cm^{-1}, $\rho = 0.0014(4)$, and $N\alpha = 0.00129(2)$ $cm^3\ mol^{-1}$ for the *trans*-isomer. These two isomers exhibit very similar parameter values. The theoretical fits of χ_M and μ_{eff} vs. T for the *cis*-isomer are shown in Fig. 2 as solid lines. The theoretical curves for the *trans*-isomer are also very similar to those for the *cis*-isomer. (The difference in the calculated χ_M values for the two isomers is smaller than 6.0×10^{-6} $cm^3\ mol^{-1}$ over the whole measured temperature range.) In the analysis of **3**, a reasonable theoretical fit was also obtained, as shown in Fig. 4 as solid lines. The best-fit parameters are $g = 1.9566(8)$, $2J = -612(16)$ cm^{-1}, and $N\alpha = 0.00110(1)$ $cm^3\ mol^{-1}$. On the other hand, no satisfactory fits were obtained for **2** by using Eq. 4. This is because complex **2** displays a sharper decrease in the experimental μ_{eff} values with decreasing the temperature from 100 K, and an analysis with the HDVV Hamiltonian never reproduces such a magnetic curve. The magnetic anomaly at lower temperatures is probably due to the spin–orbital coupling at each chromium site (*vide infra*). Therefore, the calculation was performed on the data only above 100 K at the next stage. This approach gave satisfactory fits (Fig. 3 as solid lines). The best-fit parameters are $g = 2.847(10)$, $2J = -748(14)$ cm^{-1}, and $N\alpha = 0.00219(3)$ $cm^3\ mol^{-1}$.

Discussion

The calculated parameters are summarized in Table 1. Complexes **1**, **2**, and **3** showed negative $2J$ values, indicative of an antiferromagnetic interaction between six chromium atoms. The coupling constants, $|2J|$, decrease in the order **2** (748 cm^{-1}) > **3** (612 cm^{-1}) > **1** (174.7 and 176.7 cm^{-1} for *cis*- and *trans*-isomers, respectively). The antiferromagnetic couplings in these complexes are transmitted through Cr–(μ_3-chalcogen)–Cr bridges and Cr–Cr bonds, and the magnitude of the interaction depends on the difference of the chalcogen atoms and the Cr–Cr bond lengths. In a comparison of the two hydride clusters, the antiferromagnetic couplings between chromium atoms in **2** are stronger than those in **3**. Therefore, the selenido bridges mediate exchange couplings more effectively than do the sulfido bridges. The larger exchange couplings through the selenido bridges are due to a stronger delocalization of the spin density toward the bridging atoms, which can be explained by the "ABX centrosymmetrical model" proposed by Anderson.[18] The difference in the $|2J|$ values for the two selenides, **1** and **2**, should be mainly due to different interactions through the Cr–Cr bonds. Since the Cr–Cr bond distances of **2** (2.66 Å (average)) are shorter by ca. 0.15 Å than those of **1** (2.81 Å (average)),[13] the interaction through Cr–Cr bonds is stronger and chromium atoms are more strongly coupled than those in **1**. In a comparison of the sulfide **3** with the selenide **2**, the Cr–Cr bond distances in **3** (2.59 Å (average))[14] are shorter than those in the selenide **2** by ca. 0.07 Å, and the interaction through the Cr–Cr bonds in **3** should be stronger than that in **2**. Nevertheless, the $|2J|$ values for **3** are smaller and the

Table 1. Parameters Resulting from Fitting of the Magnetic Data

Compd	g	$2J$ / cm^{-1}	$N\alpha$ / $cm^3\ mol^{-1}$	ρ
1 (*cis*-isomer)	1.973(6)	−174.7(10)	0.00128(3)	0.0016(5)
(*trans*-isomer)	1.993(6)	−176.7(8)	0.00129(2)	0.0014(4)
2	2.847(10)	−748(14)	0.00219(3)	
3	1.9566(8)	−612(16)	0.00110(1)	

antiferromagnetic couplings between the chromium atoms are weaker than those in **2**. This suggests that the difference in the bridging atoms dominates the interaction through the Cr–Cr bonds.

In complex **2**, the sharp decrease in the μ_{eff} values at lower temperatures cannot be explained by using the HDVV Hamiltonian alone. For obtaining satisfactory fits for the whole experimental curve, it is necessary to take other effects into consideration. Many complexes exhibit similar drops in the μ_{eff} values, which have been interpreted by using the intermolecular antiferromagnetic couplings.[19,20] However, the sharp decrease in the μ_{eff} values for **2** cannot be due to the intermolecular interaction, because (i) a similar magnetic anomaly is not observed for the isotypic **3**, which has almost the same intermolecular distances as those of **2**, and (ii) the unusual large g value (2.847(10)) cannot be explained. It is more plausible that the μ_{eff} curve anomaly should be the result of the spin–orbital coupling at each chromium center, since it is known that this coupling effect also causes abnormal g values for some dinuclear complexes.[19–21] When an octahedral coordination environment around a metal atom is tetragonally or trigonally distorted, the energy levels of the metal d orbitals split, which leads to a coupling of the d orbitals through the resulting small energy gap, namely spin–orbital coupling. The spin–orbital coupling effect increases because the participating energy gap is smaller. In chromium complexes **1**, **2**, and **3**, the metal centers have a square pyramidal coordination environment (C_{4v} symmetry), and 3d orbital levels split into four. These energy levels are affected by the presence or absence of interstitial hydride and the difference in the chalcogen atoms. It seems conceivable that the energy levels of some 3d orbitals at one or more chromium centers in **2** lie much closer compared with **1** and **3**, and the resulting large spin–orbital coupling of **2** causes an abnormal g value and a sharper decrease in the μ_{eff} curve at lower temperatures. In the high-temperature region, however, the kT values overwhelm the energy gaps between the d orbitals, and the antiferromagnetic interaction between chromium atoms contributes to the magnetic curve much more than does the spin–orbital coupling. Thus, the $2J$ values for **2** ($-748(14)$ cm^{-1}) obtained by using the data above 100 K must not vary very much, even if the spin–orbital coupling effect is included in the analysis.

A telluride analogue of **1** [$Cr_6Te_8(PEt_3)_6$] has been reported by Steigerwald et al.[10] This cluster exhibits an apparent decrease in the μ_{eff} values only at low temperatures. The magnetic behavior from 100 K to 300 K obeys the Curie law, and the effective magnetic moment is close to 2.8 μ_B, corresponding to two unpaired spins ($S = 1$). It is noteworthy that the telluride cluster is very different magnetically from **1**, which shows a thermal variation in the μ_{eff} values over the whole measured temperature range. This may be because the Cr–(μ_3-chalcogen)–Cr bridges in the telluride cluster mediate exchange couplings more effectively and the chromium atoms are more strongly coupled than those in the selenide **1**,[18] leading to a thermal population on only the $S = 1$ ground state up to 300 K.

Bencini et al. have reported the theoretical interpretations of the magnetic susceptibilities of octahedral iron sulfide cluster complexes $[Fe_6S_8(PEt_3)_6]X_2$ ($X = BPh_4^-$, PF_6^-) by using the HDVV Hamiltonian.[3,4] In analyses of these complexes, no distinction was made between the interaction for the *cis*-iron atoms and that for the *trans*-iron centers. The $\chi_M T$ vs. T plots for the iron complexes suggest a spin transition below 80 K, and are reproduced by two curves.[3,4] In the low-temperature region, the low-spin $S = 1/2$ state has been assigned to six Fe^{III} sites, and the magnetic curves have been explained by an antiferromagnetic interaction between the iron centers ($2J = -0.78(8)$ cm^{-1}, $X = BPh_4^-$; $2J = -0.2(8)$ cm^{-1}, $X = PF_6^-$). In the high-temperature region, however, the iron complexes have been described as a mixed-valence and mixed-spin-state compound in which one intermediate-spin ($S = 3/2$), and five low-spin ($S = 1/2$) Fe^{III} sites are localized. The best-fit parameters indicate that the interaction between the low-spin centers is antiferromagnetic ($2J = -23.1(1)$ cm^{-1}, $X = BPh_4^-$; $2J = -21.2(6)$ cm^{-1}, $X = PF_6^-$) while that between the low-spin and the intermediate-spin centers is ferromagnetic ($2J = 79.0(4)$ cm^{-1}, $X = BPh_4^-$; $2J = 330.7(4)$ cm^{-1}, $X = PF_6^-$). These results contrast with the fittings of the experimental data to single curves without a spin-transition for the chromium complexes **1**, **2**, and **3**. Since the experimental data for **1**, **2**, and **3** have been reproduced by the antiferromagnetic interaction between chromium atoms over the measured temperature range, the magnetostructures are presumably different between the iron and chromium complexes.

We thank Dr. R. Kato and Dr. Y. Hosokoshi for use of the SQUID magnetometer, and Mr. H. Tsuchiya, Cryogenic Center in Tokyo Univ., for operating the SQUID magnetometer.

References

1 F. Bottomley, J. Chen, S. M. MacIntosh, and R. C. Thompson, *Organometallics*, **10**, 906 (1991).

2 A. Bencini, S. Midollini, and C. Zanchini, *Inorg. Chem.*, **31**, 2132 (1992).

3 A. Bencini, M. G. Uytterhoeven, and C. Zanchini, *Int. J. Quantum. Chem.*, **52**, 903 (1994).

4 A. Bencini, C. A. Ghilardi, S. Midollini, A. Orlandini, U. Russo, M. G. Uytterhoeven, and C. Zanchini, *J. Chem. Soc., Dalton Trans.*, **1995**, 963.

5 S. J. Yoo, Z. Hu, C. Goh, E. L. Bominaar, R. H. Holm, and E. Münck, *J. Am. Chem. Soc.*, **119**, 8732 (1997).

6 L. Noodleman, *Inorg. Chem.*, **27**, 3677 (1988).

7 L. Noodleman, *Inorg. Chem.*, **30**, 246 (1991).

8 L. Noodleman, *Inorg. Chem.*, **30**, 256 (1991).

9 A. Bencini, C. A. Ghilardi, A. Orlandini, S. Midollini, and C. Zanchini, *J. Am. Chem. Soc.*, **114**, 9898 (1992).

10 B. Hessen, T. Siegrist, T. Palstra, S. M. Tanzler, and M. L. Steigerwald, *Inorg. Chem.*, **32**, 5165 (1993).

11 C. A. Goddard, J. R. Long, and R. H. Holm, *Inorg. Chem.*, **35**, 4347 (1996).

12 A. Bencini, and D. Gatteschi, in "Electron Paramagnetic Resonance of Exchange Coupled Systems," Springer, Berlin

(1990).

13 S. Kamiguchi, H. Imoto, T. Saito, and T. Chihara, *Inorg. Chem.*, **37**, 6852 (1998).

14 K. Tsuge, H. Imoto, and T. Saito, *Bull. Chem. Soc. Jpn.*, **69**, 627 (1996).

15 in "Landolt-Börnstein," Springer-Verlag (1981), Neue Serie II/11.

16 R. A. Heintz, T. F. Koetzle, R. L. Ostrander, A. L. Rheingold, K. H. Theopold, and P. Wu, *Nature*, **378**, 359 (1995).

17 L. F. Larkworthy, and K. B. Nolan, in "Comprehensive Coordination Chemistry," ed by G. Wilkinson, R. D. Gillard, and J. A. McCleverty, Pergamon, Oxford (1987), vol. 3, pp. 701—772.

18 P. W. Anderson, in "Magnetism," ed by, Academic Press, New York (1963).

19 O. Kahn, in "Molecular Magnetism," ed by, VCH, New York (1993), pp. 9—29.

20 O. Kahn, in "Molecular Magnetism," ed by, VCH, New York (1993), pp. 103—134.

21 O. Kahn, in "Molecular Magnetism," ed by, VCH, New York (1993), pp. 31—52.